Carbohydrate Polymer Technologies and Applications 3 (2022) 100176

Contents lists available at ScienceDirect

Carbohydrate Polymer Technologies and Applications

journal homepage: www.sciencedirect.com/journal/carbohydrate-polymer-technologies-and-applications

Fish oil-in-water emulsions stabilized by soy proteins and cellulose nanocrystals

Luciana Di Giorgio, Pablo R. Salgado, Adriana N. Mauri *

Centro de Investigación y Desarrollo en Criotecnología de Alimentos (CIDCA), CONICET CCT La Plata, CIC PBA, y Facultad de Ciencias Exactas, Universidad Nacional de La Plata, 47 y 116 S/N°, (B1900JJ) La Plata, República Argentina

ARTICLE INFO

Keywords:
O/W emulsion
Soy proteins
Cellulose nanocrystals
Fish oil
Rheological properties
Emulsion stability

ABSTRACT

This work aimed to develop fish O/W emulsions using soy protein isolate (SPI) and cellulose nanocrystals (CNC) either as separate stabilising agents or in combination. The fish O/W emulsions were prepared using aqueous dispersions containing SPI and/or different concentrations of CNC at neutral pH. The effects of each component and their concentration on the microstructure, droplet size, zeta potential, rheological behaviour, and stability of the resulting emulsions during its quiescent storage at room temperature were analysed. Emulsions prepared with both SPI and CNC showed droplets with larger sizes and surface charge than those stabilized only by SPI and were more stable than those stabilized by each component separately. The concentration of CNC determined the physicochemical and rheological properties of SPI + CNC emulsions, as well as the intervening destabilization mechanisms. Emulsion stabilized by SPI + 0.1% CNC that had a high degree of initial flocculation, turned out to be the most stable during 15 days of quiescent storage at room temperature.

Introduction

A wide variety of food ingredients and products consist either entirely or partially as emulsions or have been in an emulsified state sometime during their production (Chung & McClements, 2014). Oil-in-water (O/W) emulsions are also used as delivery systems for lipophilic compounds in the development of functional foods (McClements, Decker, Park, & Weiss, 2009). Even though O/W emulsions are thermodynamically unfavourable systems, they can become kinetically stable for a reasonable time through the addition of stabilizers, such as emulsifiers, texture modifiers, weighting agents or ripening inhibitors (McClements, 2015; Singh & Ye, 2020). Those of natural origin, such as biopolymers like proteins and some polysaccharides (Nylander, Arnebrant, Cárdenas, Bos, & Wilde, 2019), food-grade insoluble solid particles (Lam, Velikov, & Velev, 2014; Tavernier, Patel, Van der Meeren, & Dewettinck, 2017), and their combinations (Evans, Ratcliffe, & Williams, 2013; Sarkar et al., 2018) have recently gained much interest.

Soy proteins have great potential to be used as food emulsifier ingredients, due to their conformational flexibility and surface hydrophobicity (Tang, 2017). They can diffuse slowly to the oil-water interface through the continuous phase due to their large molecular weight, but once at the interface can rearrange themselves to position their hydrophobic and hydrophilic groups in the lipid and aqueous phase respectively, reducing the interfacial tension and the overall free energy of the system (Loi, Eyres, & Birch, 2019). They can contribute to electrostatic and steric stabilisation due to protein-protein interactions at interfaces and to their surface charge (Lam & Nickerson, 2013). Also, insoluble soy protein nanoparticles can be adsorbed almost irreversible to the oil-water interface and stabilize the emulsions due to the high energy barrier of desorption (Jin et al., 2019; Ju et al., 2020; Naji-Tabasi, Mahdian, Arianfar, & Naji-Tabasi, 2021). However, the O/W emulsions stabilized only by soy protein isolate (SPI) had limited global stability (Di Giorgio, Salgado, & Mauri, 2019).

Cellulose nanocrystals (CNC) are rigid rod-like particles that consist of cellulose chain segments in an almost perfect crystalline, that are mainly obtained by strong acid hydrolysis of cellulose, under strictly controlled conditions of temperature, agitation and time (Di Giorgio, Martín, Salgado, & Mauri, 2020). CNC has shown interesting emulsifying properties (Angkuratipakorn, Sriprai, Tantrawong, Chaiyasit, & Singkhonrat, 2017; Li et al., 2018; Wen, Yuan, Liang, & Vriesekoop, 2014) as they have the ability to self-assemble into liquid interfaces acting as emulsion stabilizers by the formation of a rigid layer against the flocculation or coalescence of the droplets (Rayner et al., 2014; Yang et al., 2017; Zhang et al., 2020). This behaviour was greatly influenced

* Corresponding author.
E-mail address: anmauri@quimica.unlp.edu.ar (A.N. Mauri).

https://doi.org/10.1016/j.carpta.2021.100176
Received 13 May 2021; Received in revised form 3 December 2021; Accepted 9 December 2021
Available online 12 December 2021

by surface properties, morphology, size and crystallinity of these particles, as well as by the interactions they can form among the same particles and the solvent (Hedjazi & Razavi, 2018; Kalashnikova, Bizot, Bertoncini, Cathala, & Capron, 2013; Kasiri & Fathi, 2018).

Mixtures of soy proteins and cellulose nanocrystals could be used to stabilize emulsions synergistically. It is known that competitive adsorption occurs at the emulsion interface when there are differents emulsifiers in the formulation, although interactions between the components could also be established (Dickinson, 2012; Eskandar, Simovic, & Prestidge, 2007)(Dickinson, 2012; Eskandar et al., 2007). Some recent works have been described on the stabilization of emulsions with mixtures of soy proteins and cellulose nanoparticles (Wong et al., 2021; Zhang et al., 2020).

In this context, this work aimed to develop fish O/W emulsions using soy protein isolate (SPI) and cellulose nanocrystals (CNC) either as separate stabilising agents or in combination. The fish O/W emulsions were prepared using aqueous dispersions containing SPI and/or different concentrations of CNC at neutral pH. The effects of each component and their concentration on the microstructure, droplet size, zeta potential, rheological behaviour, and stability of the resulting emulsions during its quiescent storage at room temperature were analyzed.

2. Materials and methods

2.1. Materials

Fish oil was supplied by OmegaSur (Argentina). Soy protein isolate (SPI) was supplied by IFF-Nourish (Argentina) (protein content: 85 ± 2% w/w on a dry basis; N x 5.71, measured by Kjeldahl method). Cellulose nancrystals (CNC) were prepared from microcrystalline cellulose (MCC, pH 101, Sigma-Aldrich). All the other reagents used were of analytical grade.

2.2. Cellulose nanocrystals (CNC) preparation

CNC were obtained by acid hydrolysis following the methodology described by Di Giorgio et al. (2020). The microcrystalline cellulose was dispersed (1:10 w/v) in 63.5 % H_2SO_4 w/w and was kept under continuous agitation with a magnetic stirrer (DRAGONLAB OS20-Pro, China) at 350 rpm for 2 h at 45 °C. The resulting dispersion was successively washed with distilled water and centrifuged (Z 326 K HERMLE, Germany) at 4427x*g* for 15 min at 25 °C until reaching approximately pH = 4; and then dialyzed 2 days at 4 °C using 76 mm wide and 14 KDa cut-off membranes (Sigma-Aldrich). The dialysed dispersion was sonicated (VCX 750 Vibra Cellsonics materials Inc., USA) at 225W for 10 min in an ice bath. The resulting CNC aqueous dispersion (2.81 % w/w) was stored under refrigeration at 4°C until use. CNC had a "rod" shape, with ≈ 5 nm of diameter, ≈ 410 nm of length, and zeta potential = -41 mV.

2.3. Emulsion preparation

An aqueous dispersion of SPI (5 % w/v) was prepared by magnetically stirring at room temperature, and different CNC concentrations (0, 0.1, 0.2, 0.3, 0.4, 0.5, 0.75, and 1 % w/v) were added. These dispersions (pH ≅ 7) were used as aqueous phases to prepare O/W emulsions using fish oil as the lipid phase in a protein:oil ratio of 4:1 w/w, which was equivalent to an oil:water ratio of 1.25:98.75 (Di Giorgio et al., 2019). The water and oil phases were homogenized using a high-shear probe mixer Ultra-Turrax T-25 (IKA®, Werke GmbH & Co. KG, Germany) with a dispersion tool S25N-18G (rotor diameter 13.4 mm) operated at 13, 500 rpm for 90 s. Then, this coarse emulsion was homogenized using an ultrasonic homogenizer (VCX 750 Vibra-Cell, Sonics & Materials Inc., USA) with a standard tip (13 mm diameter) operated at 20 kHz and 350 W for 300 s, with pulse duration 30 s and off time 30 s. The emulsion was kept under continuous agitation in an ice bath to minimize increases in temperature during ultrasonic treatment. The resulting O/W emulsions were named as SPI + x % CNC, being x the CNC concentration used in the formulation.

Also, O/W emulsions using aqueous phases containing only CNC in the equivalent concentrations to those described above were prepared to evaluate the emulsifying and stabilizing effect of CNC in the absence of SPI.

Two individually prepared replicates were at least assayed for each condition to confirm the repeatability of the process. The freshly prepared O/W emulsions were used for the following studies.

2.4. Emulsion characterization

2.4.1. Appearance

The visual appearance of the emulsions was registered with a digital camera (Kodak M853, USA).

2.4.2. Microstructure

Each freshly prepared O/W emulsion was placed on a slide with a cover and examined with an optical microscope equipped with a Leica DC100 digital camera (Bensheim, Germany) using a 100X magnification. The ImageJ software (ImageJ, National Institutes of Health, USA) was used to determine the droplet size registered in the optical micrographs.

2.4.3. Particle size distribution and mean diameters

Size distribution, and De Broucker ($D_{4,3}=\Sigma n_i d_i^4/\Sigma n_i d_i^3$) and Sauter ($D_{3,2}=\Sigma n_i d_i^3/\Sigma n_i d_i^2$) mean diameters of particles of the emulsions (Jafari, He, & Bhandari, 2007) were determined by static light scattering (SLS) with a particle size analyzer Mastersizer 2000E (Malvern Instruments, Worcestershire, UK) at room temperature (20°C). Measurements were made in the presence and absence of sodium dodecyl sulfate (SDS, Cicarelli, Argentina). SDS was used to prevent droplet flocculation as it negatively charged protein molecules or, over time, replaced them at the interface producing electrostatic repulsion between the droplets (McClements, 2015). Emulsions (1 ml) were mixed gently with the optional addition of 1 ml of 1 % w/v SDS solution, and then they were diluted to 600 ml of water and shaken at 2000 rpm with a dispersion unit (Hydro 2000MU, Malvern Instruments, UK). The refractive indexes of the dispersed and continuous phases were 1.47 and 1.33 respectively.

Additionally, the flocculation index (FI) and the coalescence index (CI) were calculated as follows (Palazolo, Sorgentini, & Wagner, 2005)

$$FI = \left(\frac{D_{4,3\ t} - D_{4,3\ t+SDS}}{D_{4,3\ t+SDS}}\right).100 \quad (1)$$

$$CI = \left(\frac{D_{4,3\ t+SDS} - D_{4,3\ in+SDS}}{D_{4,3\ in+SDS}}\right).100 \quad (2)$$

Where: $D_{4,3t}$ (μm) is the value of $D_{4,3}$ measured at 0, 3, 5, 10, and 15 days in the absence of SDS; $D_{4,3t+SDS}$ (μm) is the value of $D_{4,3}$ measured at 0, 3, 5, 10, and 15 days in the presence of SDS; $D_{4,3in+SDS}$ (μm) is value of $D_{4,3}$ measured at 0 days in the presence of SDS.

Emulsions were characterized at 0, 3, 5, 10, and 15 days after quiescent storage at room temperature. Determinations were made in triplicate on two independent samples of each.

2.4.4. Zeta potential

Zeta potential was measured using a dynamic light scattering analyser (SZ-100 nanopartica series, Horiba, Japan) at room temperature. O/W emulsions were diluted (1:1000 v/v) with distilled water. The sample (≈ 250 uL) was injected into a disposable cell taking care that no bubbles remained, and a measurement of the particle electrophoretic mobility results in the calculated zeta potential. Ten replicates were made for each sample.

2.4.5. Global stability

Global stability of O/W emulsions was determined by measurements of backscattered light by the sample using a Vertical Scan Analyzer (Quick Scan, Coulter Corp., Miami, FL, USA) according to (Cabezas, Madoery, Diehl, & Tomás, 2012). The freshly prepared O/W emulsions were transferred into cylindrical glass test tubes. The backscattering (BS) of monochromatic light (λ = 850 nm) from the emulsions was determined as a function of the sample height (*ca.* 65 mm) at 0, 3, 5, 10, and 15 days of the quiescent storage at room temperature. Any change due to a variation of the droplet size (flocculation, coalescence) or a local variation of the volume fraction (migration phenomena: creaming, sedimentation) was detected (Pan, Tomás, & Añón, 2002). Clarification-flocculation and coalescence-flocculation kinetics were determined recording the mean values of backscattering as a function of quiescent storage time in the lower part of the test tube (10-15 mm from the base) and in the upper part of the same (45-50 mm from the base) respectively. Determinations were conducted at least in duplicate.

2.4.6. Rheological behaviour

Rheological characterization of the freshly prepared O/W emulsions was performed in a Rheostress 600 rheometer (Thermo-Haake, Karlsruhe, Germany) with a serrated plate-plate geometry (35 mm diameter, 1 mm gap). The sample (≈ 500 uL) of the freshly prepared O/W emulsion was carefully poured onto the bottom plate of the rheometer. The top plate was slowly lowered until the gap was 1 mm. The excess sample was then removed from the edges of the plate. The sample was maintained at 25 ± 0.5 °C by a circulating water bath (Circulator DC50 Thermo-Haake) connected to the jacket surrounding the sensor system during testing. Rotational and oscillatory assays were carried out in triplicate.

Rotational test: Samples were subjected to a logarithmic increasing shear rate with a continuous ramp from 1 s^{-1} to 500 s^{-1} in 120 s, followed by a steady shear at 500 s^{-1} for 60 s, and finally a decreasing shear rate from 500 s^{-1} to 1 s^{-1} in 120 s. Flow behaviour of emulsions was described by fitting the experimental results to the Ostwald de Waele model:

$$\tau = kD^n \quad (3)$$

Where: τ is the shear stress (Pa), D is the shear rate (s^{-1}), k is the consistency index (Pa.s^n) and n is the flow behaviour index (dimensionless).

In addition, thixotropy was determined as the hysteresis area between the ascending and descending τ vs. D curves, using the RheoWin Data Manager version 4.3.0.0 software (Haake, Germany).

Oscillatory test: The region of linear viscoelasticity was determined by carrying out a stress sweep between 0.5 and 100 Pa, at a fixed frequency (= 1 Hz). Subsequently, a frequency sweep between 0.1 and 10 Hz was performed at a fixed stress (= 5 Pa, within the linear viscoelasticity range). The storage modulus (G), loss modulus (G), complex viscosity (η*) and tan delta (tg δ=G/G) were recorded as a function of frequencies.

2.5. Statistical analysis

Results were expressed as mean ± standard deviation and were subjected to analysis of variance (ANOVA). Means were tested with Tukey's HSD test for paired comparison, with a significance level α=0.05, using the Statgraphics Plus version 5.1 software (Statgraphics, USA).

3. Results and discussion

3.1. Appearance and microstructure of fish O/W emulsions

The visual appearance and the microstructure of freshly prepared fish O/W emulsions are shown in Figure 1. O/W emulsions stabilized only by CNC had a whitish colouration (see the inserts in Figure 1.I-1.O) like CNC dispersion (Di Giorgio et al., 2020), while O/W emulsions stabilized by SPI + CNC had a very faint yellowish colouration (see the inserts in Figure 1.A-1.H) attributed to SPI (Salgado, Fernández, Drago, & Mauri, 2011). However, these colour differences were not significant in the emulsions appearance.

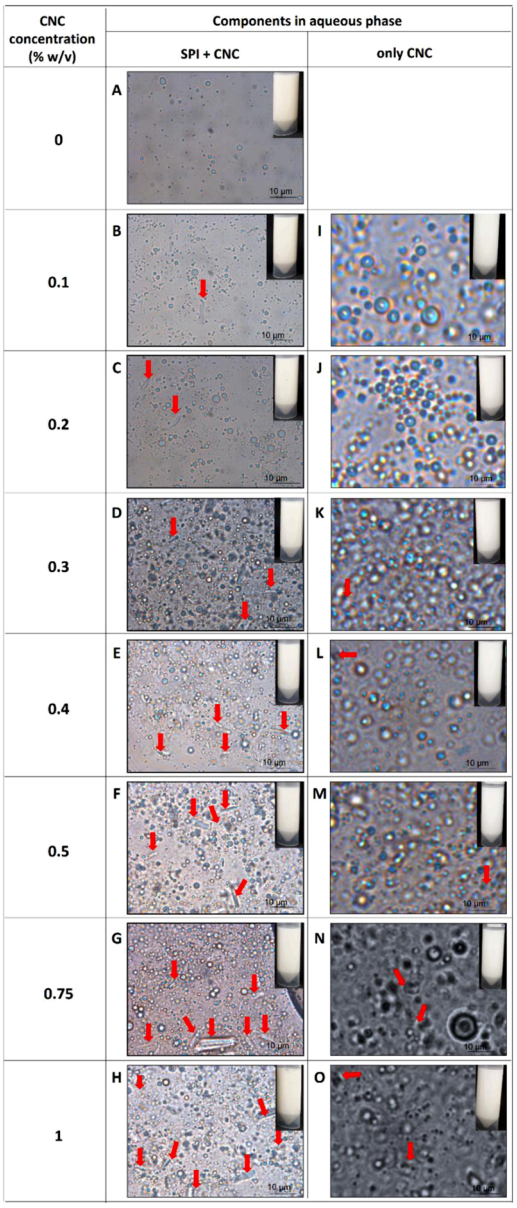

Fig. 1. Micrographs of freshly prepared fish O/W emulsions stabilized with SPI and different CNC concentrations (SPI + CNC) in the aqueous phase, and those stabilized with aqueous dispersions with different CNC concentrations but without SPI (only CNC). CNC concentrations studied: 0, 0.1, 0.2, 0.3, 0.4, 0.5, 0.75, and 1% w/v. Magnification: 100X. Red arrows point to CNC aggregates. Inserts are photographs of each O/W emulsion.

Optical micrographs showed that all emulsions presented a droplet size polydispersity (Figure 1). Oil droplets in SPI + 0 % CNC emulsion (Figure 1.A) were significantly smaller than those prepared with dispersions containing only CNC in different concentrations (only CNC; Figure 1.I-1.O) (1-3 µm vs. 15-25 µm, respectively). CNC aggregates appeared in the micrographs as elongated structures near the droplets (pointed with red arrows in Figure 1.K-1.O) at CNC concentrations equal or greater than 0.3 % w/v (Di Giorgio et al., 2020;

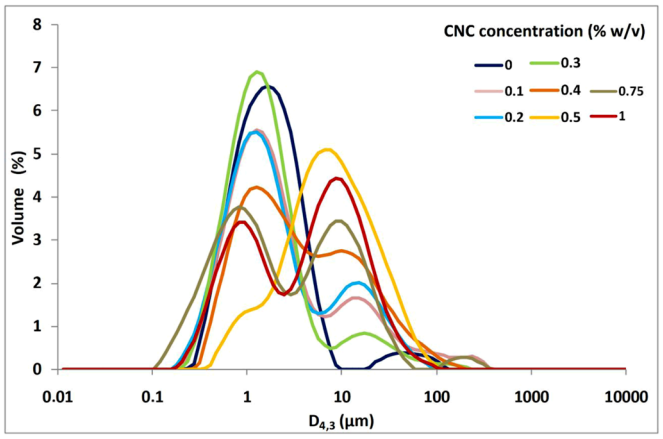

Fig. 2. Particle size distribution of freshly prepared fish O/W emulsions stabilized with SPI + CNC, using different CNC concentrations (0, 0.1, 0.2, 0.3, 0.4, 0.5, 0.75 and 1% w/v) in the aqueous dispersions.

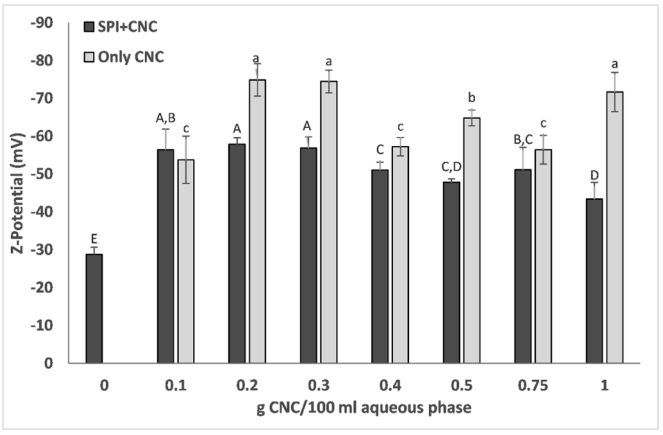

Fig. 3. Zeta potential of freshly prepared fish O/W emulsions stabilized with SPI and different CNC concentrations (SPI + CNC,) in the aqueous phase, and those stabilized with aqueous dispersions with different CNC concentrations but without SPI (only CNC,).
Bars with different letters are significantly different ($p < 0.05$) according to Tukey's test. Uppercase letters indicate differences between SPI + CNC emulsions and lowercase letters indicate differences between only CNC emulsions.

Table 1
$D_{3,2}$, $D_{4,3}$ with and without SDS, and flocculation index (FI) of freshly prepared fish O/W emulsions stabilized with SPI + CNC, using different CNC concentrations in the aqueous dispersions.

CNC concentration (% w/v)	$D_{3,2}$ (μm)	$D_{4,3}$ (μm)	FI	
	without SDS	**without SDS**	**with SDS**	
0	1.03 ± 0.17^{a}	3.60 ± 1.39^{a}	2.35 ± 0.53^{a}	53
0.1	$1.18 \pm 0.06^{a,b}$	10.17 ± 2.05^{c}	$4.26 \pm 0.61^{a,b}$	139
0.2	$1.14 \pm 0.06^{a,b}$	$6.65 \pm 1.61^{a,b,c}$	$3.95 \pm 0.28^{a,b}$	68
0.3	0.97 ± 0.11^{a}	$4.34 \pm 0.81^{a,b}$	3.05 ± 2.43^{a}	42
0.4	1.53 ± 0.29^{c}	8.55 ± 3.21^{c}	$5.87 \pm 1.19^{b,c}$	46
0.5	3.11 ± 0.34^{d}	9.85 ± 2.67^{c}	7.62 ± 0.48^{c}	29
0.75	0.99 ± 0.03^{a}	$7.39 \pm 2.20^{b,c}$	6.63 ± 2.06^{c}	12
1	$1.38 \pm 0.13^{b,c}$	$7.34 \pm 0.52^{b,c}$	7.24 ± 0.77^{c}	1

The values in the columns with different letters are significantly different ($p < 0.05$) according to the Tukey's test.

Elazzouzi-Hafraoui et al., 2008). On the other hand, all the emulsions prepared with both SPI and CNC in the aqueous phase (SPI + CNC) showed similar droplet sizes than SPI + 0 % CNC (1-3 μm) and the presence of CNC aggregates (pointed with red arrows in **Figure 1.B-1.H**), whose amount increased with CNC concentration.

3.2. Particle size distribution of fish O/W emulsions

Fig. 2 shows the particle size distributions of freshly prepared fish O/W emulsions stabilized with SPI and different concentrations of CNC (SPI + CNC) in the aqueous dispersions. All of them showed multimodal particle size distributions. The SPI + 0% CNC emulsion had a bimodal distribution, characterized by a majority population of particles with 3–4 μm diameter and a minority population around 80 μm. In SPI + 0.1% CNC emulsion, three populations were observed, the majority corresponding to particles with 1–2 μm diameter, another with sizes of 10–20 μm which could become overlapped with a third minority population that would include particles of up to 150 μm. The SPI + 0.2% CNC emulsion showed an increase in the 10–20 μm peak at the expense of that corresponding to larger diameters. In the SPI + 0.3% CNC emulsion, the population of 1–2 μm became the highest to the detriment of that of 10–20 μm. At higher CNC concentrations, the population of particles with diameters between 10 and 15 μm gradually increased in detriment of that of smaller ones until both peaks reached equivalent populations, with maximums corresponding to diameters of 1 μm and 8–10 μm, in the SPI + 0.75% CNC emulsion.

Table 1 shows the $D_{3,2}$ and $D_{4,3}$ mean diameters and the flocculation index (FI) of freshly prepared fish O/W emulsions stabilized with SPI + CNC. The $D_{3,2}$ values is inversely related to the average surface area of droplets created during emulsification, while the $D_{4,3}$ values represent the percentage of the total oil volume that is part of each of the droplets size ranges of the distribution (McClements, 2015). The SPI + 0% CNC emulsion had $D_{3,2}$ = 1 μm and $D_{4,3}$ = 3,6 μm; while all the SPI + CNC emulsions presented $D_{3,2}$ = 1–3 μm and $D_{4,3}$ = 4–10 μm (Table 1). It is known that $D_{4,3}$ is sensitive to the presence of large particles within a polydisperse system (McClements, 2015), therefore its determination was made in the presence and absence of SDS. Measurements in the presence of SDS allowed the evaluation of individual particles size, avoiding their flocculation (McClements, 2015). The comparison of both $D_{4,3}$ values (with and without SDS) (Table 1) showed that all emulsions presented flocs.

The flocculation index (FI) of SPI + 0% CNC emulsion was 53, so its individual particle size was around 2.35 μm. The SPI + 0.1% CNC emulsion presented the highest flocculation degree (FI = 139) although their individual particle size did not present significant differences with that stabilized only by SPI. But increasing CNC concentration, a less tendency to flocculation was observed, as FI decreased from 139 to 1 (Table 1). For instance, SPI + CNC emulsions with CNC concentrations greater than 0.4% presented larger individual particles (between 5.8 and 7.6 μm). In particular, the SPI + 1% CNC emulsion would be composed of a smaller number of particles of large size with a low proportion of flocs.

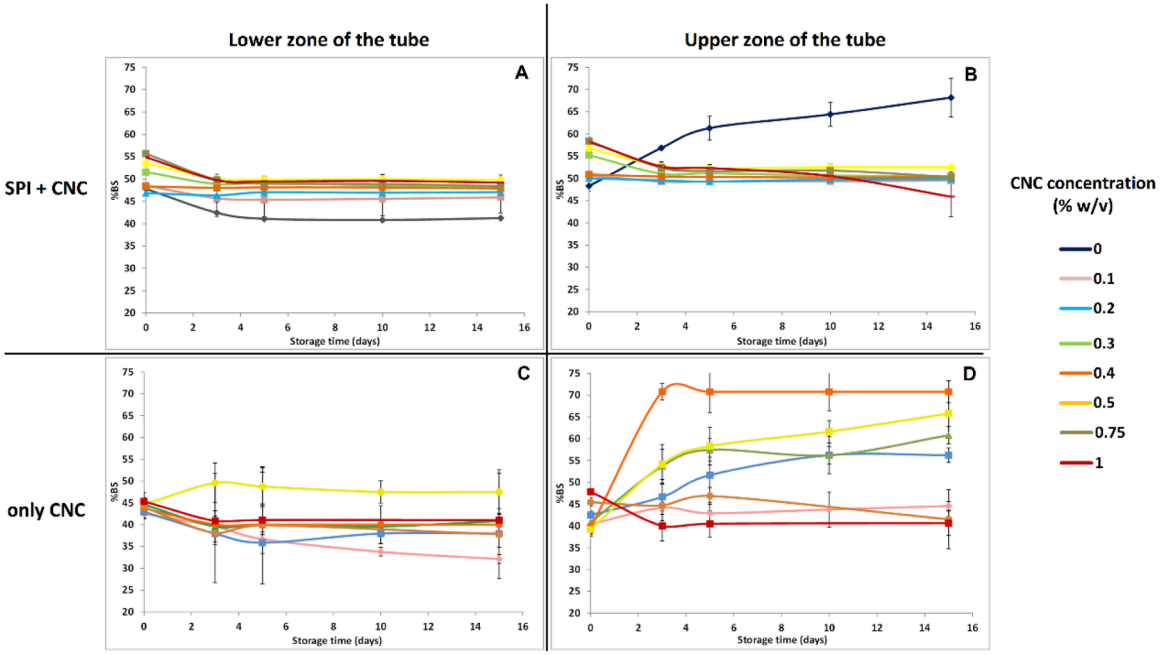

Fig. 4. Evolution of backscattering (%BS) in the clarification-flocculation zone (lower zone of the tube) (A and C) and in the coalescence-flocculation zone (upper zone of the tube) (B and D) corresponding to fish O/W emulsions stabilized with SPI and different CNC concentrations (SPI + CNC) in the aqueous phase (A and B), and those stabilized with aqueous dispersions with different CNC concentrations but without SPI (only CNC) (C and D), during their quiescent storage at room temperature. CNC concentrations studied: 0 -●-, 0.1 -●-, 0.2 -●-, 0.3 -●-, 0.4 -●-, 0.5 -●-, 0.75 -●-, and 1 -●-% w/v.

3.2. Stability of fish O/W emulsions

3.2.1. Potential zeta

Emulsions generally contain electrically charged particles that interact with each other and with the environment in which they are. Zeta potential determination allows to study these interactions and provides a measure of the net charge on the surface of the particles and the distribution of the electric potential at the interface, which finally influence the stability of the emulsion (Hunter, 2013). **Figure 3** shows the zeta potential of freshly prepared fish O/W emulsions stabilized with SPI and different CNC concentrations in the aqueous phase (SPI + CNC), and those prepared with aqueous dispersions with different CNC concentrations but without SPI (only CNC). All the emulsions showed negative zeta potential values as in the working conditions (pH≈7) soy proteins were above their isoelectric point (pI≈4.5) (Malhotra & Coupland, 2004) and CNC were functionalized with sulfate groups on their surface as a result of the acid hydrolysis conditions used to their preparation (Di Giorgio et al., 2020). Emulsions stabilized only by CNC showed zeta potential values between -54 mV and -75 mV, not finding a clear trend with CNC concentration. Values reported in this work were in the range of those described by Kargar, Fayazmanesh, Alavi, Spyropoulos, & Norton (2012) (≈ -60 mV) for O/W emulsions stabilized by CNC prepared from microcrystalline cellulose. As was expected, SPI + CNC emulsions presented higher absolute values of zeta potential than that only stabilized by SPI (SPI + 0 % CNC) (-28.8 mV) due to the high contribution in negative charge given by CNC, but lower than those stabilized only by CNC. No significant changes were observed in zeta potential values (-56 mV) of the SPI + CNC emulsions when incorporating up to 0.3 % CNC, but above this concentration zeta potential values decreased significantly to -43 mV for the highest CNC concentration. These results suggested the interactions between both components and/or the formation of CNC aggregates, that were observed in **Figure 1**. In this sense, Sarkar et al. (2017) reported a positive zeta potential value for emulsions stabilized by whey protein isolate (WPI) at pH=3, which turned negative with the addition of CNC; and postulated that CNC formed a layer around the surface of WPI coated droplets. In SPI + CNC emulsions, electrostatic interactions among the remaining positively charged domains of soy proteins and the negative ones of sulfate groups of CNC would be formed, but these electrostatic interactions seemed to be conditioned to CNC concentration

Although all the studied emulsions showed absolute zeta potential values close to or greater than 30 mV, that would indicate a good stability (Hunter, 2013), the emulsions global stability during its quiescent storage at room temperature was evaluated through backscattering analysis (Palazolo et al., 2005).

3.2.2. Global stability

The global stability of fish O/W emulsions was determined by backscattered light measurements. Fig. 4 shows the evolution of backscattering (% BS) in the clarification-flocculation zone (lower zone of the tube) (**A** and **C**) and in the coalescence-flocculation zone (upper zone of the tube) (**B** and **D**) corresponding to fish O/W emulsions prepared with SPI and different CNC concentrations (SPI + CNC) in the aqueous phase (**A** and **B**), and those prepared with aqueous dispersions with only different CNC concentrations (**C** and **D**) during its quiescent storage at room temperature. **Table S1** (Supplementary Material) also shows the mean values of the initial backscattering percentage (% BS_0) in the lower and upper zones of the tested tube for all the studied emulsions.

The SPI + 0% CNC emulsion (Fig. 4.**A** and 4.**B**) showed an uniform% BS_0 throughout the tube (≈ 48%; **Table S1**) but on the third day, it showed destabilization signs by clarification and/or flocculation through the decrease in the mean% BS of the lower zone of the tube (associated with a decrease in droplets density due to the gravitational separation) and its increase in the upper zone of the tube due to the formation of a cream phase enriched in oil droplets. From the fifth day of storage, only a slightly increasing trend in the mean%BS of the upper zone of the tube (% BS ≈ 68%) was observed; but even so no phase separation was evidenced during the 15 days of storage.

Emulsions stabilized only by CNC (**Figure 4.C and 4.D**) also presented uniform % BS_0 throughout the tube (≈ 43 %; **Table S1**), slightly lower than the SPI ones suggesting smaller droplets in SPI emulsions than those in CNC emulsions, according to optical microscopies

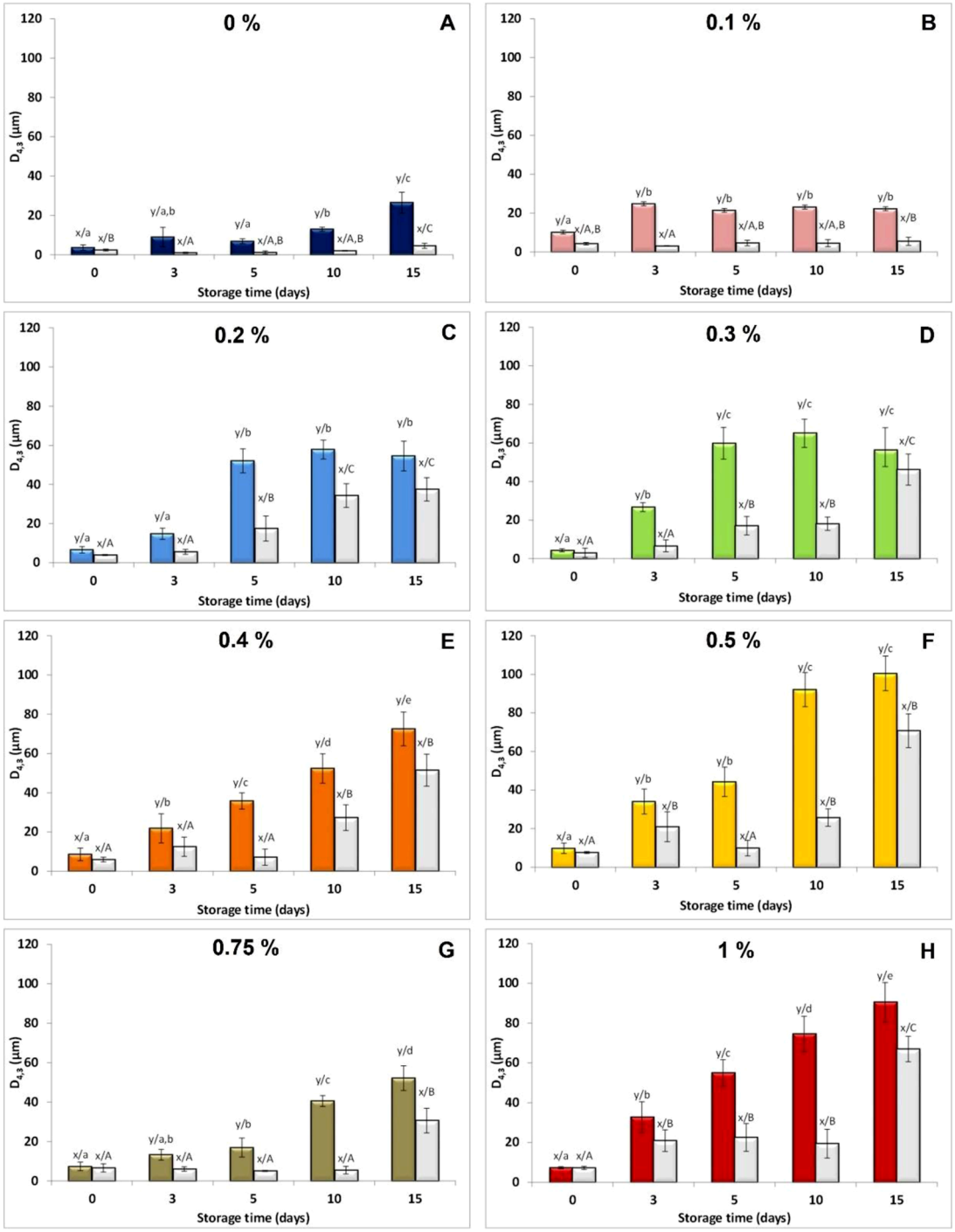

Fig. 5. $D_{4,3}$ with and without SDS of fish O/W emulsions stabilized with SPI and different CNC concentrations (SPI + CNC) in the aqueous phase, at 0, 3, 5, 10, and 15 days of quiescent storage at room temperature. CNC concentrations studied: 0, 0.1, 0.2, 0.3, 0.4, 0.5, 0.75, and 1% w/v.
Bars with different letters are significantly different ($p < 0.05$) according to Tukey's test. Letters x, y report differences between the $D_{4,3}$ value with and without SDS of each sample. Lowercase letters indicate differences between $D_{4,3}$ without SDS, and uppercase letters indicate differences between $D_{4,3}$ with SDS.

(Figure 1). CNC concentration did not significantly affect % BS_0, but it did affect emulsion stability. Emulsions formulated with extreme CNC concentrations (0.1, 0.75, and 1% CNC) were the most stable during storage, with no changes observed in their backscattering profiles (Figure 4.**C** and 4.**D**), while those with intermediate concentrations (0.2 - 0.5 % CNC) showed an increase in the mean % BS of in the upper zone of the tube suggesting that flocculation and/or coalescence mechanisms seemed to be the most important in their destabilization. Other authors that used CNC prepared from different sources to stabilize O/W emulsions in similar concentrations to the ones used in this work (Kargar et al., 2012, Kasiri & Fathi, 2018, Wang et al., 2016; Angkuratipakorn, Sriprai, Tantrawong, Chaiyasit, & Singkhonrat, 2017), indicated that in these concentrations CNC managed to cover the surface of the droplets forming a thick interfacial layer around them (Frelichowska, Bolzinger, & Chevalier, 2010).

Emulsions stabilized by SPI + CNC had higher% BS_0 than those stabilized only by CNC and similar to SPI ones except for those with 0.5, 0.75, and 1% CNC that showed the highest%BS_0 values (**Table S1**). CNC

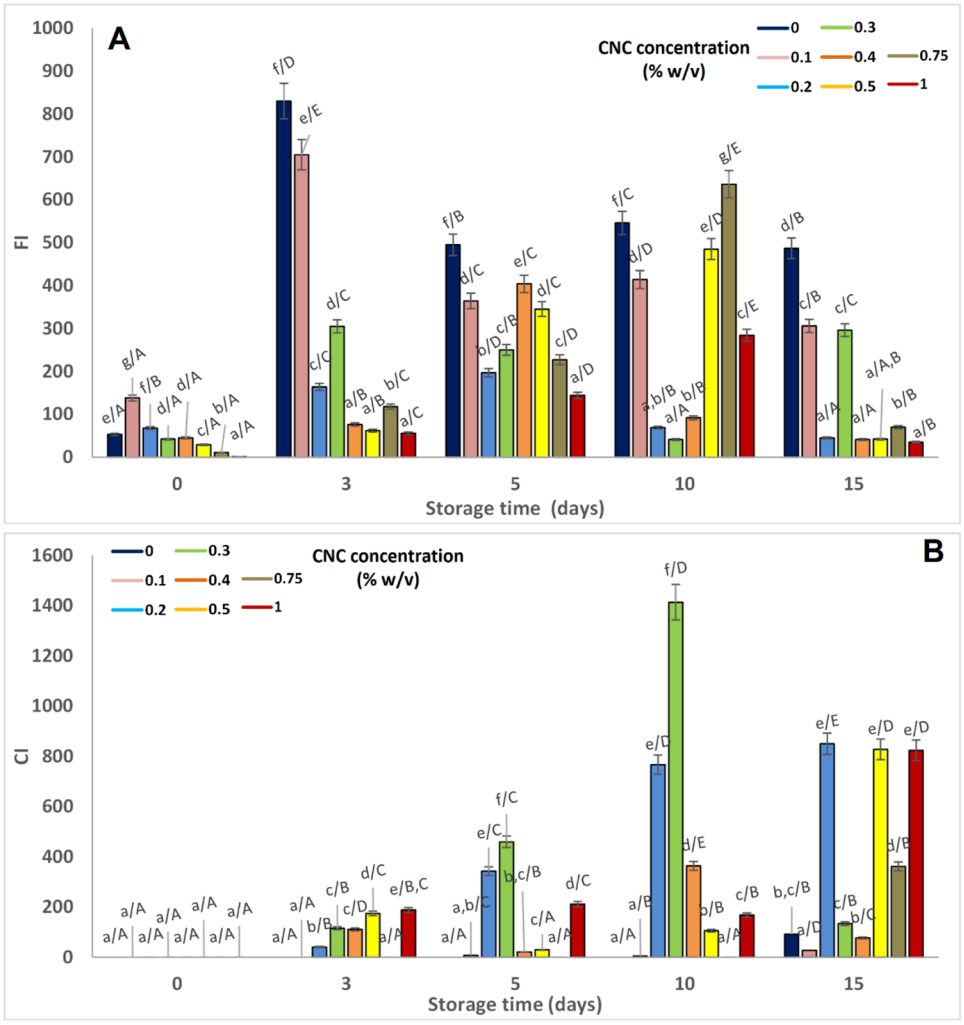

Fig. 6. (A) Flocculation index (FI) and B) coalescence index (CI) of fish O/W emulsions stabilized with SPI and different CNC concentrations (SPI + CNC) in the aqueous phase, at 0, 3, 5, 10 and 15 days of quiescent storage at room temperature. CNC concentrations studied: 0, 0.1, 0.2, 0.3, 0.4, 0.5, 0.75, and 1% w/v.
Lowercase letters indicate significant differences between the SPI + xCNC emulsions at the same time. Uppercase letters indicate significant differences of each SPI + xCNC emulsion at different storage times.

concentration affected the stability of these systems. The SPI + CNC emulsions with lower CNC concentrations (0.1, 0.2, 0.3, and 0.4%) remained stable during storage, with no changes in the mean of%BS in both zones of the tube (Fig. 3.**A** and 3.**B**). Meanwhile those containing 0.5, 0.75, and 1% CNC started to destabilize through clarification-flocculation and flocculation-coalescence from the third day of storage, showing a noticeable decrease of% BS in both zones of the tube that then remained approximately constant until the end of storage (Fig. 3.**C** and 3.**D**). Although, these systems presented an exudate liquid layer in the lower part of the tube on the fifteenth day of storage.

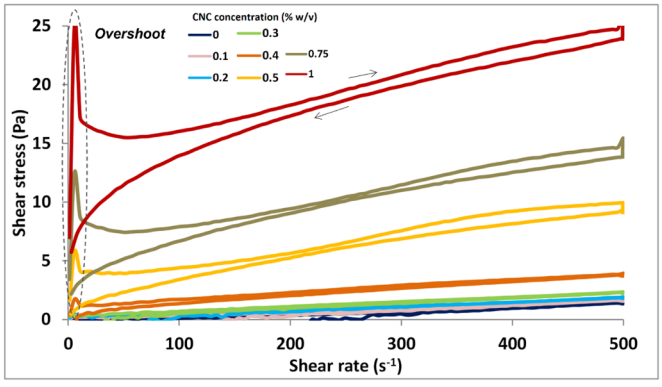

Fig. 7. Flow behaviour curves (τ vs. D) obtained by rotational tests of freshly prepared fish O/W emulsions stabilized with SPI + CNC, using different CNC concentrations (0, 0.1, 0.2, 0.3, 0.4, 0.5, 0.75, and 1% w/v) in the aqueous dispersions.

3.2.3. *Evolution of the flocculation and coalescence indexes*

The volume-weighted mean diameters ($D_{4,3}$ and $D_{4,3t+SDS}$) (Fig. 5), flocculation index (FI, Fig. 6.**A**), and coalescence index (CI, Fig. 6.**B**) of the SPI + CNC emulsions were determined as a function of the storage time. These emulsions showed an increase in their $D_{4,3}$ value during the storage time, but the increasing magnitude depended on both CNC concentration and the emulsion destabilization process. In the SPI + 0% CNC emulsion, $D_{4,3}$ increased as a function of the storage time, while $D_{4,3+SDS}$ remained approximately constant (Fig. 5.**A**), evidencing an increase of flocculation degree over time (Fig. 6.**A**). In this system, coalescence became important at the end of storage (Fig. 6.**B**), suggesting that flocs formation could delay the destabilization process.

The SPI + 0.1% CNC emulsion showed an initial increase in $D_{4,3}$ value after three days of storage which then remained constant while $D_{4,3+SDS}$ did not change throughout storage (Fig. 5.**B**). This emulsion would be composed of small particles with an initial high degree of flocculation that increased until the fifth day of analysis (Fig. 6.**A**), after which a small increase in the coalescence index was seen (Fig. 6.**B**).

The SPI + 0.2 - 0.3% CNC emulsions showed an initial increase in $D_{4,3}$ value until the fifth day of storage, which then kept constant while $D_{4,3+SDS}$ increased continuously (Fig. 5.**C** and 5.**D**). In these systems, which presented lower FI than the SPI + 0.1% CNC emulsion (Fig. 6.**A**), coalescence became more important from the third day of storage

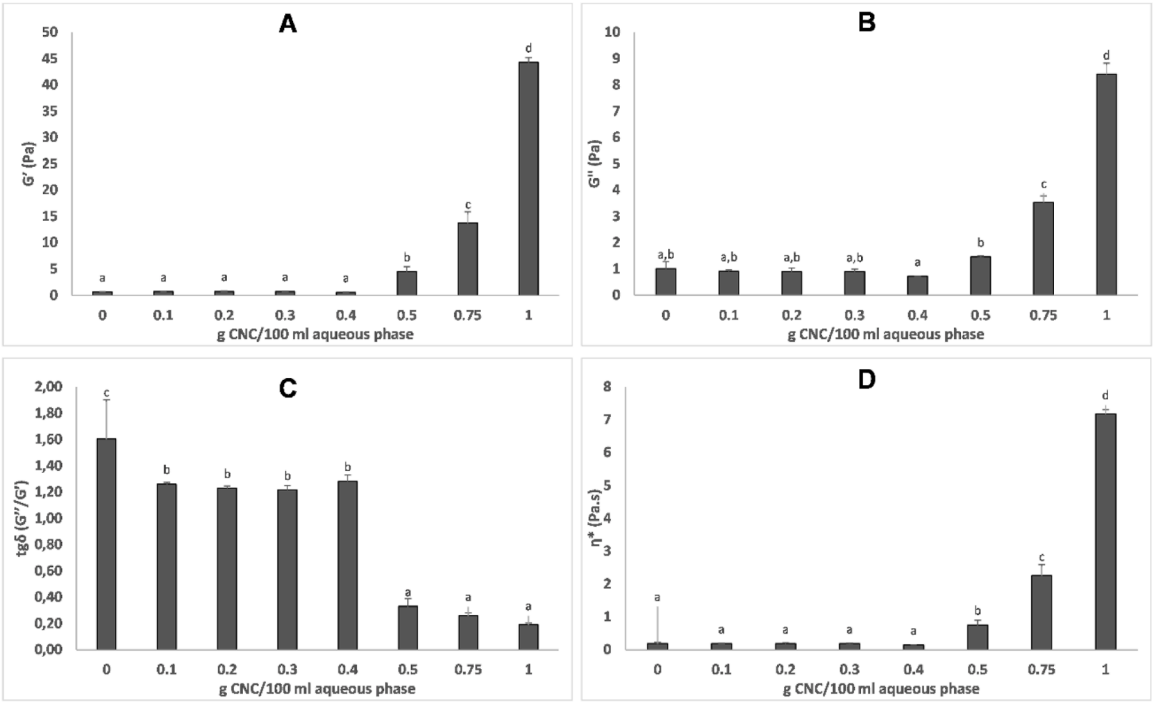

Fig. 8. (A) Storage modulus (G'), B) loss modulus (G''), C) tan delta (tg δ), and D) complex viscosity (η*) of freshly prepared fish O/W emulsions stabilized with SPI + CNC, using different CNC concentrations in the aqueous dispersions. Measurements were performed at a fixed frequency (= 1 Hz).

(Fig. 6.**B**).

The SPI + 0.4% CNC, SPI + 0.5% CNC, and SPI + 1% CNC emulsions showed a sustained increase in both, $D_{4,3}$ and $D_{4,3+SDS}$ values during storage (Fig. 5.**E**, 5.**F**, and 5.**H**). Coalescence would be their predominant destabilization mechanism, as flocculation degrees remained low (Fig. 6.**A** and 6.**B**). On the other hand, the SPI + 0.75% CNC emulsion exhibited a different behaviour; as $D_{4,3}$ steadily increased during storage while $D_{4,3+SDS}$ remained approximately constant (Fig. 5.**G**), suggesting that the flocculation mechanism would be predominant over coalescence, which was evidenced at the end of storage (Fig. 6.**A** and 6.**B**).

3.3. Rheological behaviour of fish O/W emulsions

3.3.1. Rotational analysis

Figure 7 shows the flow curves of freshly prepared SPI + CNC emulsions and **Table S2** (Supplementary Material) shows the rheological parameters that arose from the fitting of the experimental results with the Ostwald de Waele model ($r^2 > 0.97$ in all cases). Three different rheological behaviours could be distinguished according to CNC concentration. The SPI + 0 - 0.1 % CNC emulsions resulted in Newtonian fluids (n = 1) with low viscosity values and thixotropy (**Table S2**). The CNC addition produced an increase in the viscosity of these emulsions. McClements (2015) attributed this behaviour to droplets charges, explaining that when a droplet moves through a fluid, the cloud of counterions that surround it is distorted. This explanation would be valid for the SPI + 0.1 % CNC, considering that this emulsion presented higher viscosity and zeta potential than SPI + 0 % CNC one.

The SPI + 0.2 - 0.3% CNC emulsions showed pseudoplastic flow behaviour ($n<1$), increasing the consistency index and the thixotropy by increasing CNC concentration (**Table S2**). Pseudoplastic flow is the most common type of non-ideal behaviour shown by food emulsions (McClements, 2015). This behaviour could be attributed to the altered spatial distribution of particles produced by shear stress, to the facilitated alignment of non-spherical particles in the flow direction, to the association of solvent molecules with particles or to deformation and breakage of flocs by shear stress that reduces their hydrodynamic radius (Hunter, 1993; Macosko & Mewis, 1994).

Flow curves of SPI + CNC emulsions with more than 0.4 % CNC showed a sharp increase of shear stress, followed by an abrupt decrease with increasing shear rate in the low values zone (0 - 25 s^{-1}), known as "overshoot", that could be related to the formation of microstructures in the emulsion and their subsequent destruction. In this sense, Chen et al. (2011) described a partial breakdown and a rearrangement of the structures of adsorbed solid particles at the oil-water interface. The presence of an overshoot in flow curves did not allow their mathematical fitting to the selected model, suggesting that these emulsified systems had viscoelastic characteristics.

All emulsions showed thixotropy (**Table S2**). The SPI + 0 % CNC emulsion presented a low thixotropy value, as shear could cause a progressive deformation and breakdown of aggregated particles (flocs), thus decreasing their viscosity over time. Thixotropy increased progressively with CNC addition. Three-dimensional networks could be formed in SPI + CNC emulsions as a result of interactions between SPI and CNC but mainly between the CNC themselves, which could be partially or totally broken by the application of shear stress (Chen et al., 2011). Increasing CNC concentration would favour the formation of denser networks, with higher consistency and thixotropy (Peng et al., 2018). This greater structuring in SPI emulsions with 0.5, 0.75, and 1 % CNC was also manifested in the overshoot at their respective flow curves (**Figure 7**) and better studied through oscillatory tests.

3.3.2. Oscillatory analysis

Figure S1 (Supplementary Material) shows the frequency dependence of storage (G') and loss (G'') moduli for the freshly prepared SPI + CNC emulsions, and **Figure 8** summarizes the rheological parameters obtained. **Figure S1.A** shows the mechanical spectrum of the SPI + 0 % CNC emulsion, where G′ was above than G″ and that both increase with frequency. For a frequency of 1 Hz, this emulsion had G′ = 0.6 Pa, G″ = 1.0 Pa, and a phase angle (δ) of 58° (**Figure 8**). These results indicated that in this formulation the viscous properties were dominant compared to the elastic ones. In the mechanical spectra of SPI + 0.1 - 0.4 % CNC emulsions, G′ and G″ curves were almost overlapping and increased with

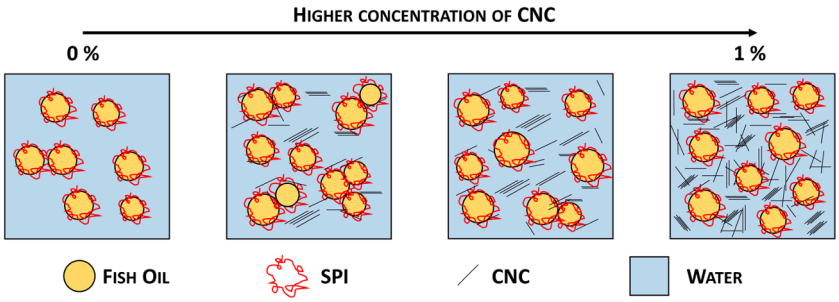

Fig. 9. Schematic representation of freshly prepared fish O/W emulsions stabilized by SPI and different CNC concentrations, integrating the results discussed in this manuscript.

frequency (**Figure S1.B-S1.E**), without showing significant differences in G′, G″and tan δ with increasing CNC concentration (**Figure 8**). In these cases, δ = 50° implied that the material responded with viscous and elastic components in equal magnitude (Chhabra & Richardson, 2011). Finally, in the mechanical spectra of SPI + 0.5 - 1% CNC emulsions, G″ was above G′, being both frequency independent. This characteristic behaviour responds to samples with a certain degree of structuring or gel-type (Masalova, Foudazi, & Malkin, 2011)., The values of both moduli increased while tan δ decreased from 18° to 11° with CNC concentration (**Figure 8**). In these formulations, the elastic properties prevailed over the viscous ones, indicating that these emulsions would have a higher degree of packaging than those previously analyzed. These three-dimensional networks with a higher degree of structuring would act like a solid when the applied stress was not sufficient to destabilize the interactions between soy proteins and CNC and between CNC themselves. In this sense, Angkuratipakorn et al. (2017) described a gel-like behaviour for rice O/W emulsions stabilized with CNC, a non-ionic surfactant and gum arabic, that attributed to a great packaging between the surfactant and both stabilizers.

Figure 8 also shows the complex viscosity (η*) of SPI + CNC emulsions. The SPI + 0 - 0.4 % CNC emulsions did not show significant differences in their η*. But from 5% CNC addition, η* increased significantly and progressively. These results evidenced the effect that CNC concentration exerted on the rheological behaviour of emulsions stabilized by both, SPI and CNC, favouring the formation of a more reinforced three-dimensional network as increasing CNC concentration.

3.4. Global analysis and possible stabilization mechanisms of SPI + CNC emulsions

The addition of CNC to emulsions stabilized by SPI seemed to increase the stability of the resulting systems (SPI + CNC). These fish O/W emulsions presented better initial characteristics and greater stability than those stabilized only by SPI (SPI + 0% CNC) or ony by CNC. Emulsions with a high degree of flocculation were obtained with low CNC concentration (SPI + 0.1% CNC), which remained stable during storage at room temperature. By increasing CNC concentration to 0.3 or 0.4% CNC, particles would be in dispersion and interactions between them would be possible, allowing flocculation and/or coalescence. Above these concentrations, the gel-like behaviour of the resulting emulsions hindered flocculation and clarification; the reason why these systems were destabilized mainly by coalescence.

It seemed that in the studied emulsions both SPI and CNC would be positioned at the oil-water interface, facilitating the formation of stable flocs when low CNC concentrations were used. But as the concentration of CNC in the emulsions increased, the interfacial film would thicken, lose its flexibility, and also increase the electrostatic repulsion. These facts would make flocculation difficult and facilitate the emulsions coalescence. Finally, when the CNC concentration was high, a three-dimensional network would be formed that would further hinder the movement of the particles and their flocculation, resulting in emulsions susceptible to coalescence. Fig. 9 presents a schematic representation of freshly prepared fish O/W emulsions stabilized by SPI and different CNC concentrations, integrating the results discussed in this manuscript.

4. Conclusion

Fish O/W emulsions using soy protein isolate (SPI) and cellulose nanocrystals (CNC) either as separate stabilising agents or in combination were studied. All SPI + CNC emulsions were more stable than those stabilized by both components separately. They presented particles with larger sizes and surface charge than those stabilized only by SPI, suggesting that the presence of cellulose nanocrystals could induce rearrangements in soy proteins, either at the oil-water interface or within the continuous phase, favouring a certain degree of interaction between both components.

CNC concentration determined the physicochemical and rheological properties of SPI + CNC emulsions, as well as the intervening destabilization mechanisms. Emulsion stabilized by SPI + 0.1% CNC, wich had a high degree of initial flocculation, turned out to be the most stable during 15 days of quiescent storage at room temperature. These emulsions could be used as delivery systems of lipophilic active ingredients such as omega-3 fatty acids from fish oil (with proven health benefits) in functional foods, amongst other applications.

Author contributions

LDG carried out the experiments. LDG, PRS and ANM analysed the data, wrote the paper, and had primary responsibility for the final content. All authors read and approved the final manuscript.

Declaration of Competing Interest

The authors declare that there are no conflicts of interest associated with this manuscript

Acknowledgements

The authors are thankful to the National Agency of Scientific and Technological Support (PICT-2013–2124; PICT-2015–2822; PICT 2018–4040, PICT 2019–3550) and the Universidad Nacional de La Plata (11/X618; 11/X750; 11/X923) for their financial support.

Supplementary materials

Supplementary material associated with this article can be found, in the online version, at doi:10.1016/j.carpta.2021.100176.

References

Angkuratipakorn, T., Sriprai, A., Tantrawong, S., Chaiyasit, W., & Singkhonrat, J. (2017). Fabrication and characterization of rice bran oil-in-water Pickering emulsion

stabilized by cellulose nanocrystals. *Colloids and Surfaces A: Physicochemical and Engineering Aspects, 522*, 310–319.
Cabezas, D. M., Madoery, R., Diehl, B. W. K., & Tomás, M. C. (2012). Emulsifying properties of hydrolized sunflower lecithins by phospholipases A2 of different sources. *Food industrial processes-methods and equipment*. InTech.
Chen, J., Vogel, R., Werner, S., Heinrich, G., Clausse, D., & Dutschk, V. (2011). Influence of the particle type on the rheological behavior of Pickering emulsions. *Colloids and Surfaces A: Physicochemical and Engineering Aspects, 382*(1), 238–245.
Chhabra, R. P., & Richardson, J. F. (2011). *Non-Newtonian flow and applied rheology: Engineering applications*. Butterworth-Heinemann.
Chung, C., & McClements, D. J. (2014). Structure–function relationships in food emulsions: Improving food quality and sensory perception. *Food Structure, 1*(2), 106–126.
Di Giorgio, L., Martín, L., Salgado, P. R., & Mauri, A. N. (2020). Synthesis and conservation of cellulose nanocrystals. *Carbohydrate Polymers, 238*, Article 116187.
Di Giorgio, L., Salgado, P. R., & Mauri, A. N. (2019). Encapsulation of fish oil in soybean protein particles by emulsification and spray drying. *Food Hydrocolloids, 87*, 891–901.
Dickinson, E. (2012). Use of nanoparticles and microparticles in the formation and stabilization of food emulsions. *Trends in Food Science & Technology, 24*(1), 4–12.
Elazzouzi-Hafraoui, S., Nishiyama, Y., Putaux, J.-. L., Heux, L., Dubreuil, F., & Rochas, C. (2008). The Shape and Size Distribution of Crystalline Nanoparticles Prepared by Acid Hydrolysis of Native Cellulose. *Biomacromolecules, 9*(1), 57–65.
Eskandar, N. G., Simovic, S., & Prestidge, C. A. (2007). Synergistic effect of silica nanoparticles and charged surfactants in the formation and stability of submicron oil-in-water emulsions. *Physical Chemistry Chemical Physics, 9*(48), 6426–6434.
Evans, M., Ratcliffe, I., & Williams, P. A. (2013). Emulsion stabilisation using polysaccharide–protein complexes. *Current Opinion in Colloid & Interface Science, 18*(4), 272–282.
Frelichowska, J., Bolzinger, M.-. A., & Chevalier, Y. (2010). Effects of solid particle content on properties of o/w Pickering emulsions. *Journal of Colloid and Interface Science, 351*(2), 348–356.
Hedjazi, S., & Razavi, S. H. (2018). A comparison of Canthaxanthine Pickering emulsions, stabilized with cellulose nanocrystals of different origins. *International Journal of Biological Macromolecules, 106*, 489–497.
Hunter, R. J. (1993). *Introduction to modern colloid science* (Vol. 7). Oxford University Press Oxford.
Hunter, R. J. (2013). *Zeta potential in colloid science: Principles and applications*. Academic press. Vol. 2.
Jafari, S. M., He, Y., & Bhandari, B. (2007). Role of Powder Particle Size on the Encapsulation Efficiency of Oils during Spray Drying. *Drying Technology, 25*(6), 1081–1089.
Jin, B., Zhou, X., Guan, J., Yan, S., Xu, J., & Chen, J. (2019). Elucidation of stabilizing pickering emulsion with jackfruit filum pectin-soy protein nanoparticles obtained by photocatalysis. *Journal of Dispersion Science and Technology, 40*(6), 909–917.
Ju, M., Zhu, G., Huang, G., Shen, X., Zhang, Y., Jiang, L., et al. (2020). A novel pickering emulsion produced using soy protein-anthocyanin complex nanoparticles. *Food Hydrocolloids, 99*, Article 105329.
Kalashnikova, I., Bizot, H., Bertoncini, P., Cathala, B., & Capron, I. (2013). Cellulosic nanorods of various aspect ratios for oil in water Pickering emulsions. *Soft matter, 9*(3), 952–959.
Kargar, M., Fayazmanesh, K., Alavi, M., Spyropoulos, F., & Norton, I. T. (2012). Investigation into the potential ability of Pickering emulsions (food-grade particles) to enhance the oxidative stability of oil-in-water emulsions. *Journal of Colloid and Interface Science, 366*(1), 209–215.
Kasiri, N., & Fathi, M. (2018). Production of cellulose nanocrystals from pistachio shells and their application for stabilizing Pickering emulsions. *International Journal of Biological Macromolecules, 106*, 1023–1031.
Lam, R. S. H., & Nickerson, M. T. (2013). Food proteins: A review on their emulsifying properties using a structure–function approach. *Food Chemistry, 141*(2), 975–984.
Lam, S., Velikov, K. P., & Velev, O. D. (2014). Pickering stabilization of foams and emulsions with particles of biological origin. *Current Opinion in Colloid & Interface Science, 19*(5), 490–500.
Li, X., Li, J., Gong, J., Kuang, Y., Mo, L., & Song, T. (2018). Cellulose nanocrystals (CNCs) with different crystalline allomorph for oil in water Pickering emulsions. *Carbohydrate polymers*.
Loi, C. C., Eyres, G. T., & Birch, E. J. (2019). Protein-Stabilised Emulsions. In L. Melton, F. Shahidi, & P. Varelis (Eds.), *Encyclopedia of food chemistry* (pp. 404–409). Oxford: Academic Press.
Macosko, C. W., & Mewis, J. (1994). *Suspension rheology*.
Malhotra, A., & Coupland, J. N. (2004). The effect of surfactants on the solubility, zeta potential, and viscosity of soy protein isolates. *Food Hydrocolloids, 18*(1), 101–108.
Masalova, I., Foudazi, R., & Malkin, A. Y. (2011). The rheology of highly concentrated emulsions stabilized with different surfactants. *Colloids and Surfaces A: Physicochemical and Engineering Aspects, 375*(1–3), 76–86.
McClements, D. J. (2015). *Food emulsions: Principles, practices, and techniques*. CRC press.
McClements, D. J., Decker, E. A., Park, Y., & Weiss, J. (2009). Structural design principles for delivery of bioactive components in nutraceuticals and functional foods. *Critical Reviews in Food Science and Nutrition, 49*(6), 577–606.
Naji-Tabasi, S., Mahdian, E., Arianfar, A., & Naji-Tabasi, S. (2021). Nanoparticles fabrication of soy protein isolate and basil seed gum (Ocimum bacilicum L.) complex as pickering stabilizers in emulsions. *Journal of Dispersion Science and Technology, 42*(5), 633–640.
Nylander, T., Arnebrant, T., Cárdenas, M., Bos, M., & Wilde, P. (2019). *Protein/emulsifier interactions. in food emulsifiers and their applications* (pp. 101–192). Springer.
Palazolo, G. G., Sorgentini, D. A., & Wagner, J. R. (2005). Coalescence and flocculation in o/w emulsions of native and denatured whey soy proteins in comparison with soy protein isolates. *Food Hydrocolloids, 19*(3), 595–604.
Pan, L. G., Tomás, M. C., & Añón, M. C. (2002). Effect of sunflower lecithins on the stability of water-in-oil and oil-in-water emulsions. *Journal of Surfactants and Detergents, 5*(2), 135–143.
Peng, J., Calabrese, V., Veen, S. J., Versluis, P., Velikov, K. P., Venema, P., et al. (2018). Rheology and microstructure of dispersions of protein fibrils and cellulose microfibrils. *Food Hydrocolloids, 82*, 196–208.
Rayner, M., Marku, D., Eriksson, M., Sjöö, M., Dejmek, P., & Wahlgren, M. (2014). Biomass-based particles for the formulation of Pickering type emulsions in food and topical applications. *Colloids and Surfaces A: Physicochemical and Engineering Aspects, 458*, 48–62.
Salgado, P. R., Fernández, G. B., Drago, S. R., & Mauri, A. N. (2011). Addition of bovine plasma hydrolysates improves the antioxidant properties of soybean and sunflower protein-based films. *Food Hydrocolloids, 25*(6), 1433–1440.
Sarkar, A., Ademuyiwa, V., Stubley, S., Esa, N. H., Goycoolea, F. M., Qin, X., et al. (2018). Pickering emulsions co-stabilized by composite protein/polysaccharide particle-particle interfaces: Impact on in vitro gastric stability. *Food Hydrocolloids, 84*, 282–291.
Sarkar, A., Zhang, S., Murray, B., Russell, J. A., & Boxal, S. (2017). Modulating in vitro gastric digestion of emulsions using composite whey protein-cellulose nanocrystal interfaces. *Colloids and Surfaces B: Biointerfaces, 158*, 137–146.
Singh, H., & Ye, A. (2020). Chapter 12 - Interactions and functionality of milk proteins in food emulsions. In M. Boland, & H. Singh (Eds.), *Milk proteins (Third edition) (Third edit* (pp. 467–497). Academic Press.
Tang, C.-. H. (2017). Emulsifying properties of soy proteins: A critical review with emphasis on the role of conformational flexibility. *Critical Reviews in Food Science and Nutrition, 57*(12), 2636–2679.
Tavernier, I., Patel, A. R., Van der Meeren, P., & Dewettinck, K. (2017). Emulsion-templated liquid oil structuring with soy protein and soy protein: K-carrageenan complexes. *Food Hydrocolloids, 65*, 107–120.
Wang, W., Du, G., Li, C., Zhang, H., Long, Y., & Ni, Y. (2016). Preparation of cellulose nanocrystals from asparagus (Asparagus officinalis L.) and their applications to palm oil/water Pickering emulsion. *Carbohydrate Polymers, 151*, 1–8.
Wen, C., Yuan, Q., Liang, H., & Vriesekoop, F. (2014). Preparation and stabilization of D-limonene Pickering emulsions by cellulose nanocrystals. *Carbohydrate Polymers, 112*, 695–700.
Wong, S. K., Supramaniam, J., Wong, T. W., Soottitantawat, A., Ruktanonchai, U. R., & Tey, B. T. (2021). Synthesis of bio-inspired cellulose nanocrystals-soy protein isolate nanoconjugate for stabilization of oil-in-water Pickering emulsions. *Carbohydrate Research, 504*, Article 108336.
Yang, Y., Fang, Z., Chen, X., Zhang, W., Xie, Y., Chen, Y., et al. (2017). An Overview of Pickering Emulsions: Solid-Particle Materials, Classification, Morphology, and Applications. *Frontiers in Pharmacology, 8*, 287.
Zhang, X., Luo, X., Wang, Y., Li, Y., Li, B., & Liu, S. (2020). Concentrated O/W Pickering emulsions stabilized by soy protein/cellulose nanofibrils: Influence of pH on the emulsification performance. *Food Hydrocolloids, 108*, Article 106025.